

Cu(OH)₂ nanowires, CuO nanowires and CuO nanobelts

G.H. Du, G. Van Tendeloo *

EMAT, Department of Physics, University of Antwerp, Groenenborgerlaan 171, B-2020 Antwerp, Belgium

Received 28 April 2004; in final form 1 June 2004

Available online 20 June 2004

Abstract

Cu(OH)₂ nanowires, CuO nanowires and CuO nanobelts have been prepared and their (micro)structure is characterized by X-ray diffraction, high-resolution transmission electron microscopy and electron energy loss spectroscopy. Cu(OH)₂ nanowires are formed by a self-assembly mechanism of nanocrystals. These nanocrystals tend to orient their [1 0 0] axis parallel or close to parallel with the growth direction. The diameter of the monoclinic CuO nanowires is 8–20 nm. CuO nanobelts are single crystalline; the growth direction is along the [0 1 0] direction and they lie on the (0 0 1) plane; the edge surfaces being the (1 0 0) crystal planes.

© 2004 Elsevier B.V. All rights reserved.

1. Introduction

The study of one-dimensional nanostructures is one of the most active areas due to their peculiar, fascinating physical, chemical and mechanical properties different from the bulk material. In particular, their important role as both interconnect and active component for fabricating nanoscale electronic and phonic devices has attracted attention [1–3]. Cupric oxide (CuO) is a p-type semiconductor with a narrow band gap (1.2 eV) and exhibits a number of interesting properties [4]. Copper oxide based materials have widespread applications [5–7], such as high-temperature superconductors, optical switch, anode electrodes for batteries. Recent studies indicate that CuO could exist in as many as three different magnetic phases [8,9]. CuO has also been exploited as a powerfully heterogeneous catalyst to convert hydrocarbons completely into carbon dioxide and water [10]. Several methods have been developed to prepare one-dimension nanostructures. Among these, chemical vapor deposition (CVD) [11], laser vaporization, electrochemical techniques [12,13], hydrothermal treatment [14,15] and the exfoliating method [16] have been documented. However studies about CuO nanowires and nanobelts are still limited. Recently Xia and

coworkers [17] reported the synthesis of CuO nanowires by heating copper substrates to temperatures between 400 and 700 °C. CuO nanofibers have been synthesized by Hsieh et al. [18] using a process of self-catalytic growth at 500 °C.

Here we describe a facile method to produce Cu(OH)₂ nanowires, CuO nanowires and nanobelts. No organic template and catalyst are needed and the method is suited for large-scale preparation. The microstructures of these nanoscale products are analyzed in detail using transmission electron microscopy (TEM), which allows us to propose a formation mechanism.

2. Experimental

In a typical synthesis, 1 g of Cu(NO₃)₂ is first dissolved in 100 ml distilled water. Then, 30 ml NH₃ · H₂O (0.15 M) solution is added to the Cu(NO₃)₂ solution under constant stirring. A blue precipitate of Cu(OH)₂ is produced when NaOH (1 M) solution is added dropwise to the above solution to adjust the pH value to 9–10. At last the blue Cu(OH)₂ precipitate is filtered and washed several times to obtain a solid product. The solid products are separated into three parts. One part is dried at room temperature (denoted as sample A). The second part is placed in an oven and heated at 130 °C for 10 h (denoted as sample B). The third part is added to 30 ml

* Corresponding author. Fax: +32-3-2653257.

E-mail addresses: staf.vantendeloo@ua.ac.be (G. Van Tendeloo).

distilled water and the mixture solution is sealed in a Teflon-lined stainless autoclave and kept at a temperature of 130 °C for 10 h. A black solid product is formed in the solution and separated by filtration (denoted as sample C).

Powder X-ray diffraction (XRD) analysis was performed using a Rigaku Dmax X-ray diffractometer with Cu K α radiation ($\lambda = 0.1541$ nm). The morphology and structure of the products was determined using high-resolution transmission electron microscopy (HRTEM) using a JEOL 4000EX and a Philips CM30FEG microscope. Electron energy loss spectroscopy (EELS) was performed using a Gatan Image Filtering (GIF) system attached to the Philips CM30FEG. TEM samples were prepared by dispersing the powder in alcohol by ultrasonic treatment, positioning a drop onto a porous carbon film supported on a copper grid, and then drying in air.

3. Results and discussion

Fig. 1 shows the XRD profiles taken from the sample A, B and C. The peaks in Fig. 1a can all be well indexed in the orthorhombic $\text{Cu}(\text{OH})_2$ structure with lattice constants $a = 2.951$ Å, $b = 10.59$ Å and $c = 5.273$ Å (JCPDS 35-0505). Figs. 1b,c show that both sample B and C are pure CuO with a monoclinic structure ($a = 4.685$ Å, $b = 3.425$ Å, $c = 5.13$ Å, $\beta = 99.549$, JCPDS 45-0937). The relatively broad XRD peaks in Figs. 1a,b indicate that the size of crystals in sample A and B is small. The XRD profile of sample C (Fig. 1c) shows narrow and sharp peaks in comparison with Fig. 1a,b, indicating a larger crystal size and a better crystallinity than sample A and B.

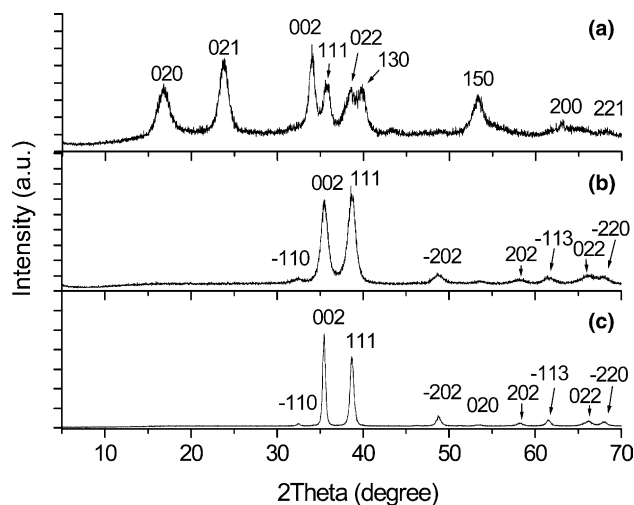


Fig. 1. XRD profiles of (a) sample A, (b) sample B and (c) sample C. Sample A was indexed as pure $\text{Cu}(\text{OH})_2$ while sample B and C could be indexed as pure CuO.

Fig. 2a is a low magnification transmission electron microscopy (TEM) image of sample A. It consists entirely of a large number of nanowires with a fairly uniform diameter of 10–20 nm. The length of nanowires varies from 500 nm to 2 μm and the purity of nanowires is as high as 98% (estimated from XRD and TEM results). Fig. 2b is a selected area electron diffraction (SAED) pattern recorded from an area containing a large number of nanowires. The rings in the pattern can be indexed as the (020), (021), (110), (111), (130), (132), (200) and (222) rings of the orthorhombic $\text{Cu}(\text{OH})_2$, in agreement with the XRD results. No extra reflections are observed and we can therefore conclude that sample A consists of pure $\text{Cu}(\text{OH})_2$ nanowires.

$\text{Cu}(\text{OH})_2$ nanowires prefer to grow into bundles, which usually have a width of 40–100 nm (Fig. 2c). A HRTEM image of a single $\text{Cu}(\text{OH})_2$ nanowire is displayed in Fig. 2d, revealing that a single $\text{Cu}(\text{OH})_2$ nanowire is actually assembled from dozens of nanocrystals with an average size of 4×9 nm. The constituting nanocrystals have an elongated shape along the direction of the longest dimension of the nanowire. In the HREM image several interplanar spacings (0.226, 0.25 and 0.28 nm) are observed, corresponding to the (130), (111) and (110) planes of $\text{Cu}(\text{OH})_2$. There seems to be no fixed orientation relationship between the different nanocrystals.

Single-crystalline nanowires in general have been extensively studied. Their formation is clearly related to the fact that the growth rate along one crystallographic direction is significantly faster than along the other directions. The situation is different however for nanowires with a polycrystalline structure, which is usually formed by the aggregation of many crystals [19]. Porous single-crystalline CaCO_3 have been prepared via nanocrystals aggregation by Zhan et al. [20] and aggregation-based crystal growth in natural iron oxyhydroxide biomineralization products has been reported by Banfield [21]. For $\text{Cu}(\text{OH})_2$ nanowires we suggest the following mechanism. First, Cu^{2+} cations in the $\text{Cu}(\text{NO}_3)_2$ solution form a square-planar complex $[\text{Cu}(\text{NH}_3)_4]^{2+}$ with the addition of $\text{NH}_3 \cdot \text{H}_2\text{O}$. When NaOH is added, the pH value of the solution increases and the stability of the $[\text{Cu}(\text{NH}_3)_4]^{2+}$ decreases. The effects of pH and $\text{NH}_3 \cdot \text{H}_2\text{O}$ on the $\text{Cu}(\text{OH})_2$ morphology have been studied by Wang et al. [22]. $\text{Cu}(\text{OH})_2$ precipitates because it is more stable than $[\text{Cu}(\text{NH}_3)_4]^{2+}$. It is conceivable that the nucleation of $\text{Cu}(\text{OH})_2$ starts from localized regions with relatively high concentrations of OH^- where the $[\text{Cu}(\text{NH}_3)_4]^{2+}$ complex is unstable. Because a large number of nuclei are formed simultaneously, many $\text{Cu}(\text{OH})_2$ nanocrystals precipitate. $\text{Cu}(\text{OH})_2$, however, is a layered structure (Fig. 2e) and the growth rate is anisotropic. Therefore the shape of the $\text{Cu}(\text{OH})_2$ nanocrystals is not spherical and they prefer a morphology with one dimension longer than the

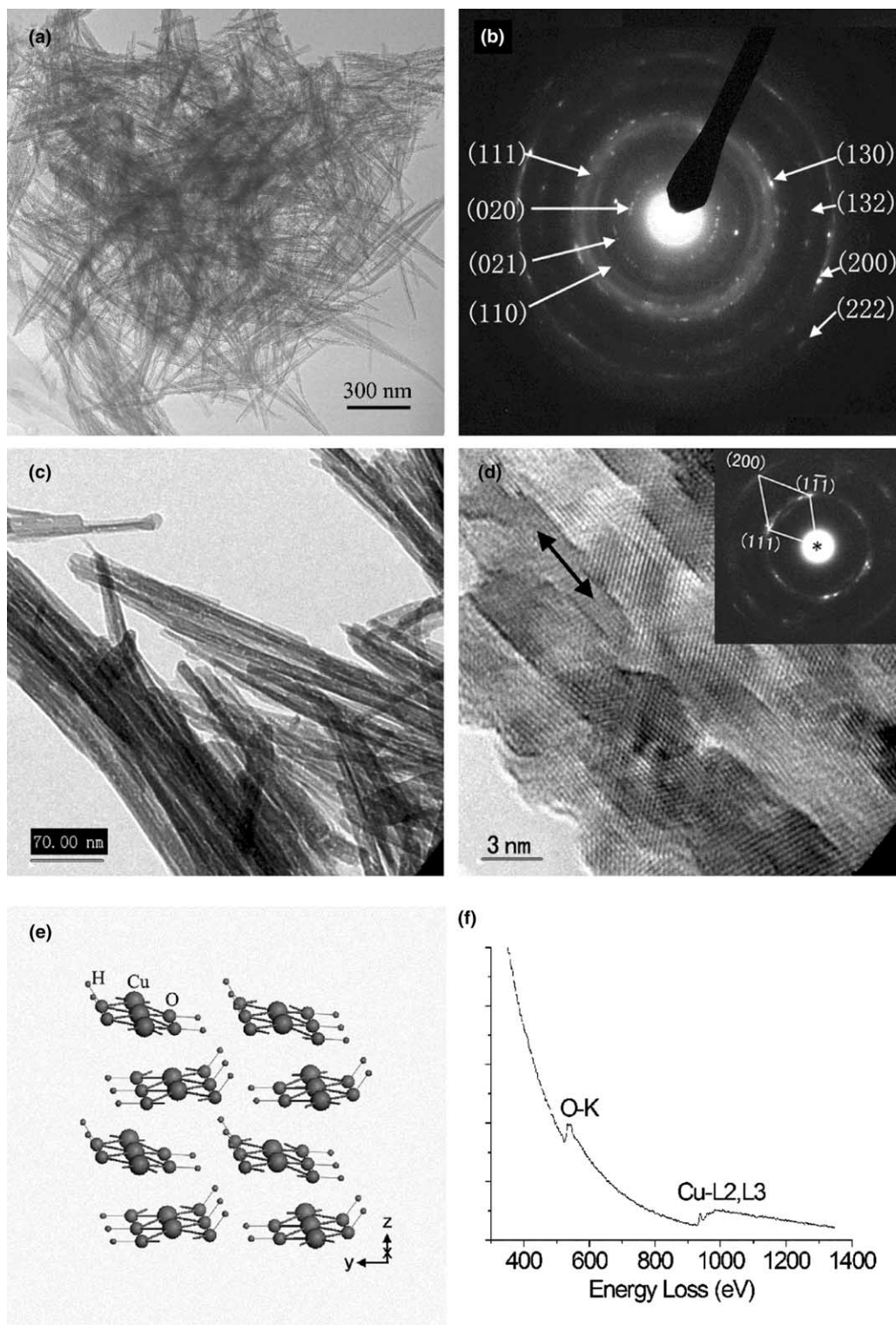


Fig. 2. (a) Low magnification TEM image of $\text{Cu}(\text{OH})_2$ nanowires, (b) SAED pattern taken from a region including a large number of nanowires, (c) TEM image of bundled $\text{Cu}(\text{OH})_2$ nanowires, (d) HRTEM image of a $\text{Cu}(\text{OH})_2$ nanowire (the arrow indicates the growth direction) and SAED pattern taken from a single nanowire (inset), (e) structure model of $\text{Cu}(\text{OH})_2$ and (f) EELS spectrum from a $\text{Cu}(\text{OH})_2$ nanowire.

others. At a certain point the nanocrystals aggregate and assemble to form nanowires.

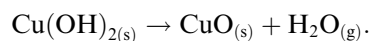
However one important question remains: why do these nanocrystals assemble to form nanowires instead of

clusters or random particles? We can get some clue from the SAED taken from a single $\text{Cu}(\text{OH})_2$ nanowire (inset in Fig. 2d). The ring pattern confirms that the nanowire is composed of many nanocrystals (polycrystalline struc-

ture). However the brightness of the diffraction ring is not uniform, indicating a preferential orientation of these nanocrystals. The angle between the two brighter spots on the $\{111\}$ diffraction ring is about 64° and they can be indexed as (111) and $(\bar{1}\bar{1}\bar{1})$ reflections. The detailed SAED experiment and crystallographic analysis indicate that there is indeed a preferential orientation and many nanocrystals tend to orient their $[100]$ direction parallel to the growth direction of the $\text{Cu}(\text{OH})_2$ nanowire. This can explain why the wire-like $\text{Cu}(\text{OH})_2$ are formed. The aggregation and assembly process of $\text{Cu}(\text{OH})_2$ nanocrystals is not random but selective. The nanocrystals of similar orientation are easy to connect and grow together; the aggregating rate along the $[100]$ direction is faster than along other directions, leading to the formation of $\text{Cu}(\text{OH})_2$ nanowires. The diameter of the nanowires is uniform mainly because the aggregating rate along these directions is very low so that the difference between them is small.

The composition of a single $\text{Cu}(\text{OH})_2$ nanowire was analyzed using EELS. Fig. 2f is a typical EELS spectrum taken from a single nanowire, clearly showing the O K edge at 532 eV, the L2 and L3 edges of Cu at 951 and 931 eV, respectively. No nitrogen (K edge is at 401.6 eV) is detected, indicating the absence of the complex $[\text{Cu}(\text{NH}_3)_4]^{2+}$ or NH_4^+ along the nanocrystalline boundaries.

TEM images of sample B are shown in Fig. 3; the morphology is very similar to sample A. A large amount of nanowires with a diameter of 8–20 nm are observed in Fig. 3a. The rings in the SAED pattern (inset of Fig. 3a) can be indexed as (-110) , (002) , (111) , $(\bar{2}02)$, (202) and (022) reflections of pure monoclinic CuO. The HRTEM image reveals that the CuO nanowires are also polycrystalline with a nanocrystal size around 3–8 nm (Fig. 3b). The boundaries between nanocrystals become vague because of the crystallization process at 130°C . The formation mechanism of the CuO nanowires is easy to understand. During the heating process, the $\text{Cu}(\text{OH})_2$ nanowires loose H_2O molecules and transform into CuO while the nanowire morphology still remains. A detailed transformation process from $\text{Cu}(\text{OH})_2$ to CuO was suggested by Cudennec and Lecert [23] and can be described according to the following scheme:



The loss of water is performed by an oxolation mechanism, which involves a dehydration process and the formation of O–Cu–O bridges (see Fig. 3c). Bridges are formed after the loss of water molecules followed by a contraction of the structure along the $[010]$ direction. Simultaneously shifts of CuO_4 groups or Cu atoms along (001) direction are performed to promote the evolution towards crystallized CuO.

A low-magnification TEM image of sample C is shown in Fig. 4a. Compared with sample A and B, sample C

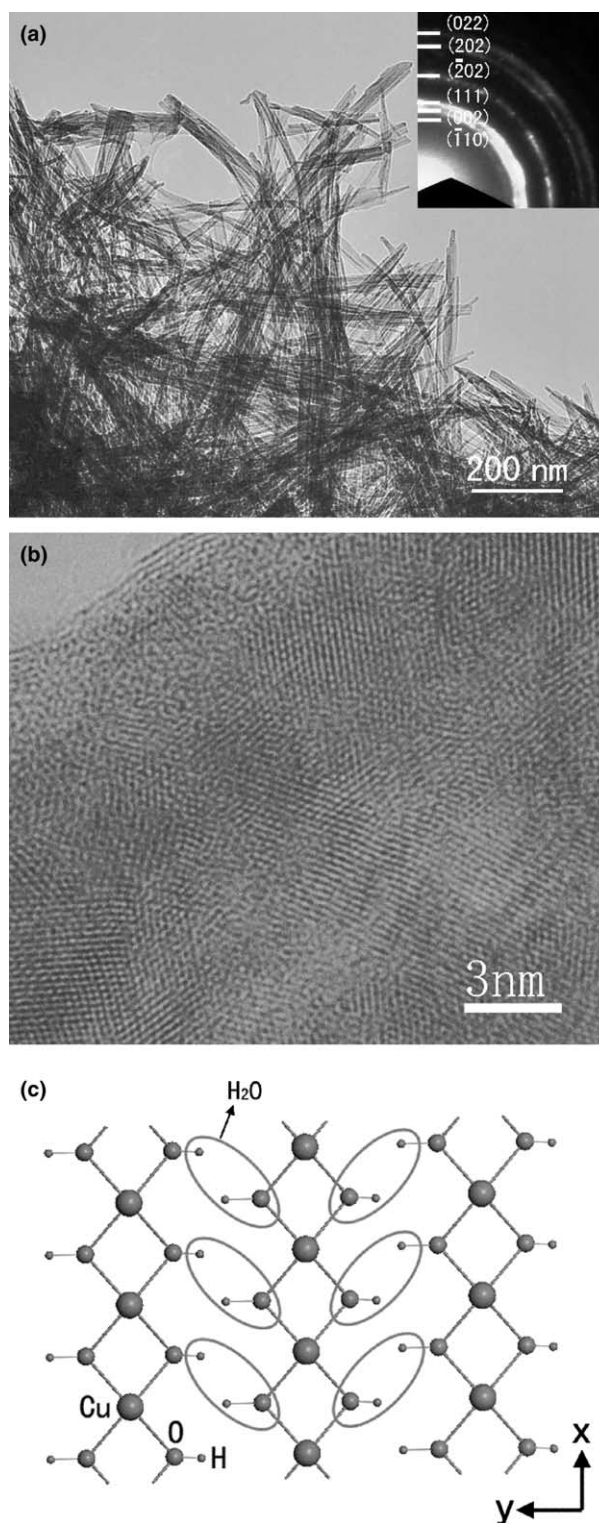


Fig. 3. (a) TEM image of CuO nanowires; the SAED pattern is shown as inset, (b) HRTEM image of a CuO nanowire and (c) structure model of $\text{Cu}(\text{OH})_2$ showing the process to loose water molecules.

shows a different morphology: a lamellar and belt-like morphology is clear. The width of the CuO belts ranges from 120 to 350 nm and the length is over $1\ \mu\text{m}$. Fig. 4b is an enlarged image of a single CuO nanobelt and the inset

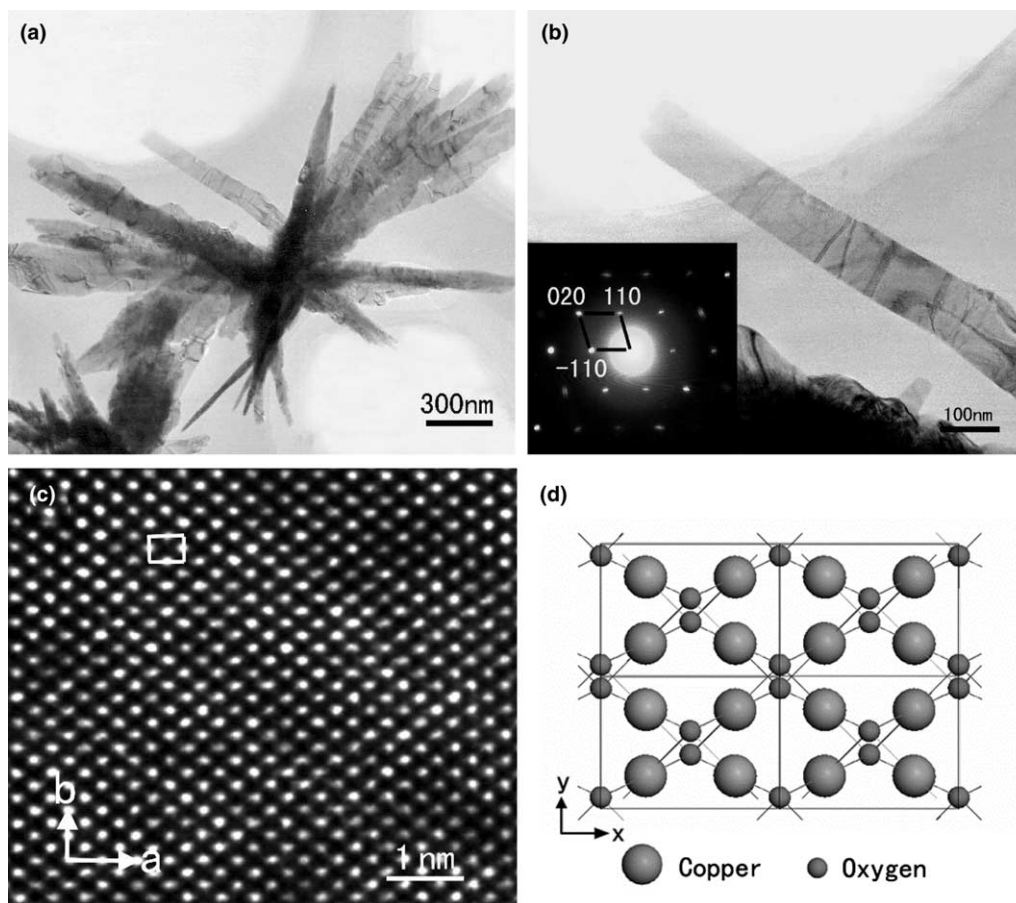
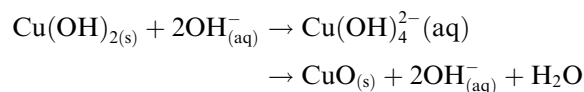


Fig. 4. (a) Low magnification TEM image of CuO nanobelts, (b) TEM image of a single CuO nanobelt with the corresponding SAED pattern as inset, (c) HRTEM image of a CuO nanobelt imaged along the [001] direction and (d) projected structure model of CuO along the [001] direction.

is the corresponding SAED pattern. The electron beam is along the [001] zone axis and the diffraction spots can be indexed as the (-110) , (110) and (020) reflections of CuO. Detailed tilt experiment and SAED demonstrate that the CuO nanobelt is single crystalline with the long axis along [010]. This is reasonable because the close-packed plane of the monoclinic CuO crystal is (010). Fig. 4c is a HRTEM image of a CuO nanobelt and it clearly shows sub unit cell detail; the projected unit cell ($a = 4.6 \text{ \AA}$ and $b = 3.4 \text{ \AA}$) is outlined. White dots in the image correspond to the open channels between four Cu-atoms. The corresponding projected structure model of CuO is shown in Fig. 4d.

TEM results suggest that the CuO nanobelts lie on (001) planes and that the edge surface is the (100) crystal plane. The formation of a CuO nanobelt is due to the processes of thermal dehydration and re-crystallization of the $\text{Cu}(\text{OH})_2$ nanowires. It is a different transformation mechanism for $\text{Cu}(\text{OH})_2$ in aqueous solutions or in the solid state [23]. Divalent copper ions are firstly dissolved under the form of complex anions $\text{Cu}(\text{OH})_4^{2-}$, which result in the a square planar surrounding. This anion can be considered as the precursor for the formation of CuO. A condensation phenome-

non, combined with a loss of two hydroxyl ions and one water molecule, lead to the formation of chains of square planar CuO_4 groups and then to solid CuO. The transformation can be described as the following scheme:



The presence of water facilitates the morphologic transformation from nanowire to nanobelt.

4. Conclusions

We report the preparation and structure investigation of $\text{Cu}(\text{OH})_2$ nanowires, CuO nanowires and nanobelts. $\text{Cu}(\text{OH})_2$ nanowires are formed by self-assembly of nanocrystals with a size of $4 \times 9 \text{ nm}$. These nanocrystals tend to orient their [100] axis parallel to the growth direction. The diameter of $\text{Cu}(\text{OH})_2$ and CuO nanowires are in the range from 5–20 nm and their length varies from 500 nm to 2 μm . The CuO nanobelts are single crystalline and lie on the (001) plane with the edge surfaces as the (100) crystal plane; the growth direction

is the [010] direction. The growth mechanism of these nanostructures is discussed. The preparation method has the advantages of relatively low cost, high purity and large-scale production, and may be extended to the synthesis of other nanostructures.

Acknowledgements

Part of this work has been supported by IAP V-1.

References

- [1] A. Bachtold, P. Hadley, T. Nakanishi, C. Dekker, *Science* 294 (2001) 1317.
- [2] Y. Huang, X.F. Duan, Y. Cui, L.J. Lauhon, K.H. Kim, C.M. Lieber, *Science* 294 (2001) 1313.
- [3] R. Martel, T. Schmidt, H.R. Shea, T. Hertel, P. Avouris, *Appl. Phys. Lett.* 73 (1998) 2447.
- [4] A.O. Musa, T. Akomolafe, M.J. Carter, *Sol. Energ. Mater. Sol. C.* 51 (1998) 305.
- [5] C. Macilwain, *Nature (London)* 403 (2000) 121.
- [6] A.H. MacDonald, *Nature (London)* 414 (2001) 409.
- [7] F. Lanza, R. Feduzi, J. Fuger, *J. Mater. Res.* 5 (1990) 1739.
- [8] J.B. Forsyth, P.J. Brown, B.M. Wanklyn, *J. Phys. C* 21 (1988) 2917.
- [9] B.X. Yang, T.R. Thurston, J.M. Tranquada, G. Shirane, *Phys. Rev. B* 39 (1989) 4343.
- [10] J.B. Reitz, E.I. Solomon, *J. Am. Chem. Soc.* 120 (1998) 11467.
- [11] Zhengwei Pan, Zurong Dai, Zhonglin Wang, *Science* 291 (2001) 1947.
- [12] Y. Zhou, S.H. Yu, X.P. Cui, C.Y. Wang, Z.Y. Chen, *Chem. Mater.* 11 (1999) 545.
- [13] J.J. Zhu, S.W. Liu, O. Palchik, Y. Kolytyn, A. Gedanken, *Langmuir* 16 (2000) 6396.
- [14] G.H. Du, Q. Chen, R.C. Che, L.M. Peng, *Appl. Phys. Lett.* 79 (2001) 3702.
- [15] G.H. Du, Q. Chen, P.D. Han, L.M. Peng, *Phys. Rev. B* 67 (2003) 035323.
- [16] G.H. Du, L.-M. Peng, Q. Chen, S. Zhang, W.Z. Zhou, *Appl. Phys. Lett.* 83 (2003) 1638.
- [17] X. Jiang, T. Herricks, Y. Xia, *Nano Lett.* 2 (2002) 1333.
- [18] C.T. Hsieh, J.-M. Chen, H.-H. Lin, H.-C. Shih, *Appl. Phys. Lett.* 82 (2003) 3316.
- [19] G.H. Du, Y.H. Wei, T. Dou, C. Iwamoto, H. Ichinose, B.S. Xu, *J. Inorg. Mater.* 15 (2000) 1073.
- [20] J.H. Zhan, H.P. Lin, C.Y. Mou, *Adv. Mater.* 15 (2003) 621.
- [21] J.F. Banfield, S.A. Welch, H.Z. Zhang, T.T. Ebert, R.L. Penn, *Science* 289 (2000) 751.
- [22] W.Z. Wang, C. Lan, Y.Z. Li, K.Q. Hong, G.H. Wang, *Chem. Phys. Lett.* 366 (2002) 220.
- [23] Y. Cudennec, A. Lecert, *Solid State Sci.* 5 (2003) 1471.